



**Analysis of the Surface Temperature and Environmental
Fragility of the Municipality of Arujá, State of São Paulo – Brazil**
Análise da Temperatura da Superfície e da Fragilidade
Ambiental do Município de Arujá, Estado de São Paulo - Brasil

Bruna Daniele de Carvalho Gimenez Torresani¹;
Anderson Targino da Silva Ferreira¹; Antonio Roberto Saad²;
William de Queiroz¹ & Fabrício Bau Dalmas¹

¹Universidade Universus Veritas Guarulhos. Programa de Mestrado em Análise Geoambiental,
Praça Tereza Cristina, 239, 07023-070, Guarulhos, SP, Brasil

²Universidade de São Paulo. Instituto de Geociências. Rua do Lago, 562 - Butantã, 05508-080, São Paulo, SP
E-mails: brunared.gimenez@gmail.com; atargino@prof.ung.br;
saadhome@uol.com.br; wqguarulhos@gmail.com; fdalmas@prof.ung.br

Recebido em: 12/11/2018 Aprovado em: 20/03/2019

DOI: http://dx.doi.org/10.11137/2019_2_07_18

Abstract

The Municipality of Arujá is located northeast of the Metropolitan Region of São Paulo (RMSP) between the Cantareira and Itapeti mountains, along the Presidente Dutra Highway (BR-116) and along the banks of the Baquirivu-Guaçu and Jaguari rivers. Because it is a municipality of significant environmental importance for the RMSP, given its still large green area, it was necessary to apply geoprocessing techniques with the objective of analyzing the potential and emergent fragility, in the sense of pointing out necessary areas of conservation and / Or environmental mitigation. However, the work showed that the potentially more fragile areas were those located in the NNE portions of the municipality. In these, the geomorphological domain of high hills associated with high slopes, pointed to the necessity of conservation of these areas, considering that these lands are still covered by large arboreal vegetation and free of urban occupation. On the contrary, the areas of the municipality located in the SSO portions, this fragility that was previously potentially low today, is presented as an emergency, mainly due to the urban occupation.

Keywords: Geoprocessing; Environmental fragilities; Surface temperature; Landsat-8

Resumo

O Município de Arujá está situado a nordeste da Região Metropolitana de São Paulo (RMSP) entre as serras da Cantareira e Itapeti, junto à Rodovia Presidente Dutra (BR-116) e às margens dos rios Baquirivu-Guaçu e Jaguari. Por se tratar de um município de significativa importância ambiental para a RMSP, haja vista sua ainda grande área verde, se fez necessário a aplicação de técnicas de geoprocessamento com objetivo analisar a fragilidade potencial e emergente, no sentido de apontar áreas necessárias de conservação e/ou mitigação ambiental. Contudo, o trabalho mostrou que as áreas potencialmente mais frágeis foram aquelas situadas nas porções NNE do município. Nessas, o domínio geomorfológico de morros altos associados a altas declividades, apontaram para a necessidade de conservação dessas áreas, tendo em vista que esses terrenos ainda se encontram cobertos por vegetação arbórea de grande porte e livres de ocupação urbana. De modo contrário, as áreas do município situadas nas porções SSO, essa fragilidade que antes era potencialmente baixa, hoje, apresenta-se emergencialmente alta devido principalmente a ocupação urbana.

Palavras-chave: Geoprocessamento; Fragilidades ambientais; Temperatura da superfície; Landsat-8

1 Introduction

Tricart (1977) concept of Ecodynamic Units involves the dynamics and energy/matter flows in the environment. Ross (1995), based on Tricart (1977), states that the synthesis products in the geographic territory and their contents must focus on the multi-themes of specialized disciplines. He defines Environmental Fragility Units as synthesis products, the natural environments being their potential fragilities and the environments that are affected by human action being their emerging fragilities, thus precisely defining the guidelines and actions to be implemented in the physical-territorial space.

Ross (1990 and 1994) defines as Stable Ecodynamic Units those units that “are in dynamic equilibrium and were protected from human action, consequently remaining in their natural state”. The Unstable Ecodynamic Units, on the other hand, are “those that have undergone intensive anthropic interventions that modified the natural environments by means of deforestation and practice of miscellaneous economic activities”. The author also defined subcategories, such as Emerging Instability for the Unstable Ecodynamic Units, from very weak to very strong, and Potential Instability for the Stable Ecodynamic Units, classified in qualitative terms.

Regarding urban environments, Santos and Ross (2012) map environmental fragility based on the principle that in these areas runoff and the possibility of infiltration and drainage after rainfall are directly related to more or less intensive local environmental fragility.

The principle that guides the preparation of environmental fragility maps is the definition of different fragility levels for the natural environments, which have or have not undergone some modification by anthropic activity (Ross, 1994). Environmental fragility mapping can be divided in: (i) Potential Fragility mapping that, as far as this research is concerned, aims to present the predisposition of the environment to factors such as geomorphology, lithology, pedology and terrain declivity as a function of the natural susceptibility of the terrain (lower areas) to flooding and the possibility of mass movements (Klais *et al.*, 2012), and (ii) Emerging

Fragility mapping, which highlights areas associated with unstable environments, where anthropogenic interventions have intensively modified the natural environment (Santos, 2015).

According to Feitosa *et al.* (2011), the constant climatic changes are the response to transformations resulting from urban expansion. Such process causes impacts on the environment, leading to environmental disequilibria. The modified space affects meteorological elements, creating different microclimates. These disequilibria are caused by the impermeabilization of the soil by means of materials that conduct and irradiate thermal energy in the urban environment.

In this sense, Voogt & Oke (2003) point out that urban climatology studies focusing on Surface Temperature (ST) are extremely important, because ST modulates the air temperature (urban atmosphere) in the lower layers, controlling the energy exchange that destabilizes the urban population’s thermal comfort.

Therefore, the objective of this study is the geoenvironmental analysis of the Municipality of Arujá (State of São Paulo) by means of the preparation of Potential and Emerging Fragility maps, leading to the mapping of surface temperatures. Such analysis uses geoprocessing techniques, aiming to contribute to adequate territorial management actions regarding the municipality.

2 Study Area

According to IBGE (2018), the Municipality of Arujá is located in the São Paulo City Metropolitan Region – SPMR (Figure 1). According to the IBGE census (IBGE, 2011), the population of Arujá was estimated to be in 2010 approximately 82,651 inhabitants, with a demographic density of 779.33 inhabitants/km². The climate of Arujá is similarly to the São Paulo City Metropolitan Region, is subtropical. The mean annual temperature is 18°C, being July the coldest month (mean temperature of 14°C) and February the hottest month (mean temperature of 22°C); the mean rainfall is 1,400 mm/year (IBGE, 2018).

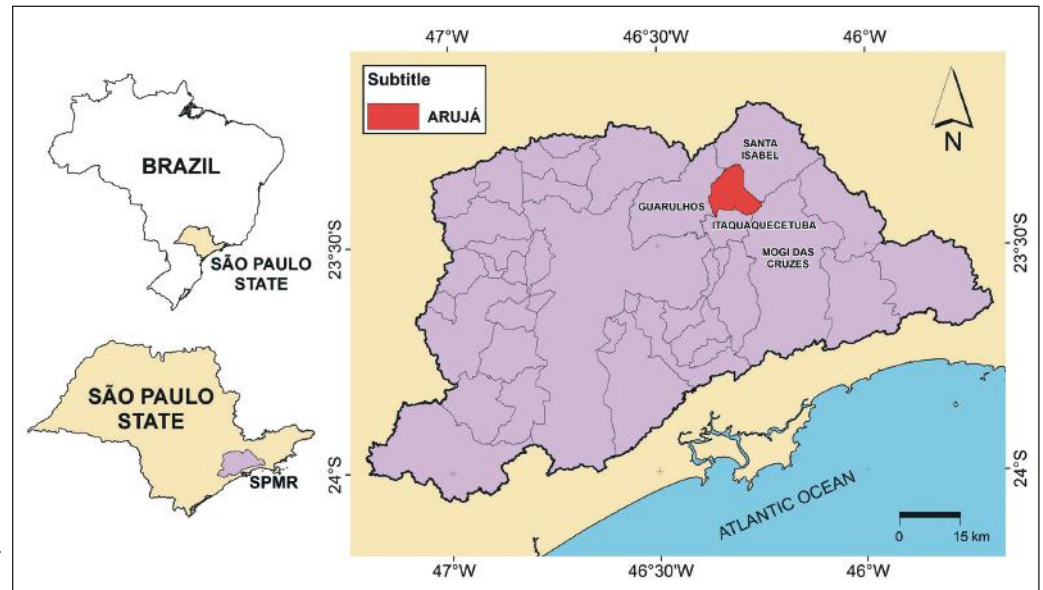


Figure 1 Location of the Municipality of Arujá in SPMR.

2.1 Land Use

The Land Use map is essential, because it represents the anthropic factor, which is largely responsible for changes in the natural landscape. According to PMA (2012), the Municipality of Arujá is 97.7 km² in area, 39.24 % of which corresponds to the Atlantic Forest. The land use classes of the study area are presented in Figure 2, where arboreal and grassy vegetation predominate, respectively with 33.78% and 33.82% of the municipality area. This percentage in the urban area is 21.81% (in 2015). To the north of the municipality the vegetation cover is largely arboreal, shrub and herbaceous and includes some agricultural activity.

The analysis of the land use map clearly shows the high level of urban consolidation in the central and southern portion of the municipality, because it is where the main (Presidente Dutra) highway is located, linking one side of the municipality to the other.

3 Methodology

After the survey of the theoretical data and the compilation of a spatial database, the following steps were performed as the methodology applied to this study: (i) preparation of thematic – fragility and thermal – maps; (ii) crossing of data, data analysis and

preparation of the Potential and Emerging Fragility maps; and (iii) analysis of the information on fragilities with the mean surface temperatures.

The spatial database was developed by means of geoprocessing techniques that involve the integration and compatibilization of data of different natures, sources, scales, dates and formats. It is composed of a cartographic base, aerial photos and other thematic information bases, systematized in geographic information system environments (ArcGIS).

3.1 Preparation of the Thematic Maps

All mapping and analyses were performed using the geographic information system ArcGIS (v. 10.2). For temperature mapping the Landsat-8 satellite image from September 23rd, 2015 was used (sensor OLI; scene and orbit 219/076; band 10 multispectral scanning, and spatial resolution of 30 meters).

In order to obtain the Surface Temperature map in °C (ST), band 10 (30-m spatial resolution) of the Thermal Infrared Sensor (TIRS) – Landsat-8, was used, which corresponds to the thermal infrared range (10.6–11.19 μm – micrometer) (USGS, 2017).

Thus, to convert the Gray Levels (GL) of each image pixel to radiance, later converted to TS (in °C), Equation 1 was applied, which is based on Table 1.

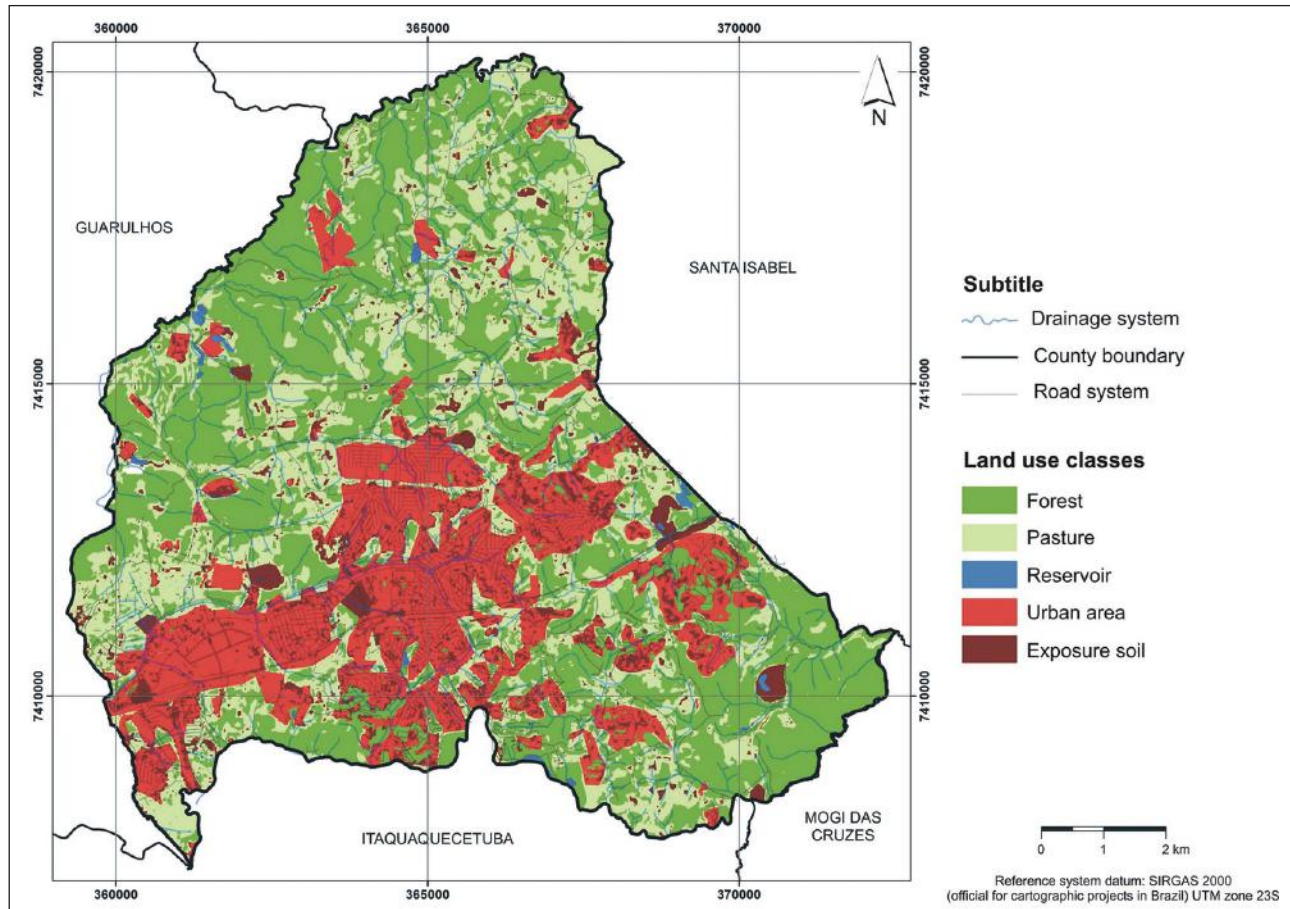


Figure 2 Land use map of the Municipality of Arujá.

NC	Radiance Values
Lλ	Spectral Radiance of the sensor in $w.m^{-2}.sr^{-1}.μm^{-1}$
ML	multiplicative resizing factor of band 10 = 3.3420E-04
AL	adding resizing factor specific for band 10 = 0.10000
Qcal	quantized value calibrated by pixel in DN = image band 10

Table 1 Elements and values used in the conversion equation to radiance extracted from Landsat-8 image band 10 metadata (USGS, 2017).

After the transformation of NC to radiance, Equation 1, which is based on Table 2, was applied, aiming to obtain TS values (°C):

$$TS (°C) = \{(K_2) / (\ln (K_1 / L\lambda + 1))\} - 273.15 \quad (1)$$

The adopted methodology follows Ross (1994) proposals adapted by Santos (2015), which resulted in an analysis for urban environments. For

NC	Radiance Values
TS (°C)	Effective Temperature in the satellite in °C
K1	Calibration constant 1 = 774.89 (K)
K2	Calibration constant 2 = 1321.08 (K)
Lλ	Spectral Radiance of the Sensor in $w.m^{-2}.sr^{-1}.μm^{-1}$

Table 2 Elements and values of the calibration constant extracted from Landsat-8 image band 10 metadata (USGS, 2017).

the preparation of the Potential Fragility Map, the database used included geologic, geomorphologic, pedologic and declivity (vector file of contour lines) information. The Emerging Fragility Map was prepared from the combination of the Potential Fragility Map and the Land Use Map of Arujá of 2015.

The application of geoprocessing techniques started with the attribution of weights to each class of the thematic maps for declivity (Table 3), geolo-

gy (Table 4), geomorphology (Table 5) and land use (Table 6). After weight attribution, all criteria (thematic maps) were standardized in the Fuzzy Overlay extension of Arc GIS, version 10 (ESRI, 2011), in a scale in bytes, from zero to one (Eastman, 2006). The multicriteria analysis was performed in the Weighted Sum extension of Arc GIS, version 10 (ESRI, 2011).

MAP	DECLIVITY CLASSES (%)	WEIGHT	CLASSIFICATION
DECLIVITY	Up to 6	1	Very Weak
	From 6 to 12	2	Weak
	From 12 to 20	3	Medium
	From 20 to 30	4	High
	Above 30	5	Very High

Table 3 Weights attributed to declivity classes.
 Source: Ross (1994), Massa & Ross (2012).

MAP	CLASSES	WEIGHT
GEOLOGY	Alluvium	3.0
	Granitoid	0.7
	Gneiss	0.7
	Metapelite	1.1
	Tertiary	1.8

Table 4 Weights attributed to geological classes.
 Source: Modified after Crepani *et al.* (2001).

MAP	CLASSES	WEIGHT
GEOMORPHOLOGY	Restricted Plain	1
	Mound	2
	Low Hill	2.5
	High Hill	3

Table 5 Weights attributed to geomorphological classes.
 Source: Modified after Silveira *et al.* (2014).

MAP	CLASSES	WEIGHT
LAND USE	Predominance of natural conditions with well-developed vegetation and/or vegetation in advanced regeneration stage favoring infiltration. Portions situated in higher areas of high declivity.	1
	Natural or artificial arboreal formations with dense grassy base. Cultivated and uncultivated pastures.	2
	Areas with water bodies.	3
	Impervious urbanized area.	4
	Urbanized area and/or area presenting exposed soil.	5

Table 6 Weights attributed to land use classes.
 Source: Adapted from Ross (1994), and Santos (2006).

4 Results and Discussions

4.1 Geomorphology

The geomorphological map prepared by the Technological Research Institute (Ross & Moroz, 1996) was improved to scale 1:50.000. The relief of the Municipality of Arujá is part of a mountainous system that separates the rain and fluvial waters of the major Tietê and Paraíba do Sul hydrographic basins. The geomorphologic features found in the Municipality of Arujá are characteristic of the Atlantic Plateau, encompassing shear faults originated from divergent plate tectonics and associated magmatic phenomena. The Arujá morphologic classification is based on the methodology proposed by Ross & Moroz (1996), and includes high hills, low hills, mounds and plains.

The areas to the east are characterized by high hills with declivities higher than 45% and amplitudes higher than 150 m. Low hills are present at the northern and southeastern extremes, with declivities up to 45% and maximum amplitude of 100 m. The mounds predominate in the central-southern region, characterized by declivity up to 30% and topographic amplitudes equal or less than 40 m. The plains predominate in the western and southern regions, presenting declivities up to 5% and amplitudes less than 10 m. When not rectified, drainage channels are sinuous, as shown in Table 7.

Relief Unit	Characteristics
Plain	Declivities up to 5% and amplitudes lower than 10 m. Sinuous drainage channels, when not rectified.
Mounds	Declivities up to 30% and topographic amplitudes up to 40 m. Dendritic to sub-parallel pattern with medium drainage density.
Low hills	Declivities up to 45% and amplitudes up to 100 m. Dendritic pattern with high drainage density.
High hills	Declivities higher than 45% and amplitude up to 150 m. Dendritic pattern with high drainage density.

Table 7 Morphological Classification of the Arujá Relief (Based in: Andrade, 2008).

4.2 Maps and Analysis of the Potential and Emerging Fragilities

It can be seen in the Potential Fragility Map of the Municipality of Arujá (Figure 3) that 55.81

km² of the territory (57.13% of the total area) are encompassed in areas of very low and low fragility. Such regions are inserted where there are evidences of arboreal cover, which is paramount for the maintenance of the landscape. Viezzer *et al.* (2016) concluded in their research that such maintenance is provided by thermal comfort, temperature decrease, shade, pollution reduction, well-being and aesthetic beauty.

The Potential Fragility Map also shows that the areas of very low and low fragility (respectively green and yellow colored) are inserted where declivity is 0-20 %, in other words, plain regions. However, these are located where consolidated urban areas predominate, thus resulting in areas with different instability degrees. Thus, authors such as Massa and Ross (2012) and Ribeiro (2016) directly relate the high values of slope and high values of fragility.

Medium fragility (orange) corresponds to 19.75 % of the area of the municipality. The major contribution to interpret this class came from the geological map, highlighting the Alluvium, Tertiary and Metapelite classes.

High (red) and very high (purple) fragilities correspond to 17.98 % and 5.14 % of the area of the municipality. The Potential Fragility Map conforms areas that are inserted in the high fragility class, which is under the direct influence of declivity and geomorphology. This is even more evident in the high declivity and high hill classes, also found in urban regions, as in the case of the southeastern portion of the municipality.

On account of different land uses, the different impact types and levels are generated so that they highlight the highest urban occupation with the lack of arboreal cover (Ribeiro, 2016). This reflects in

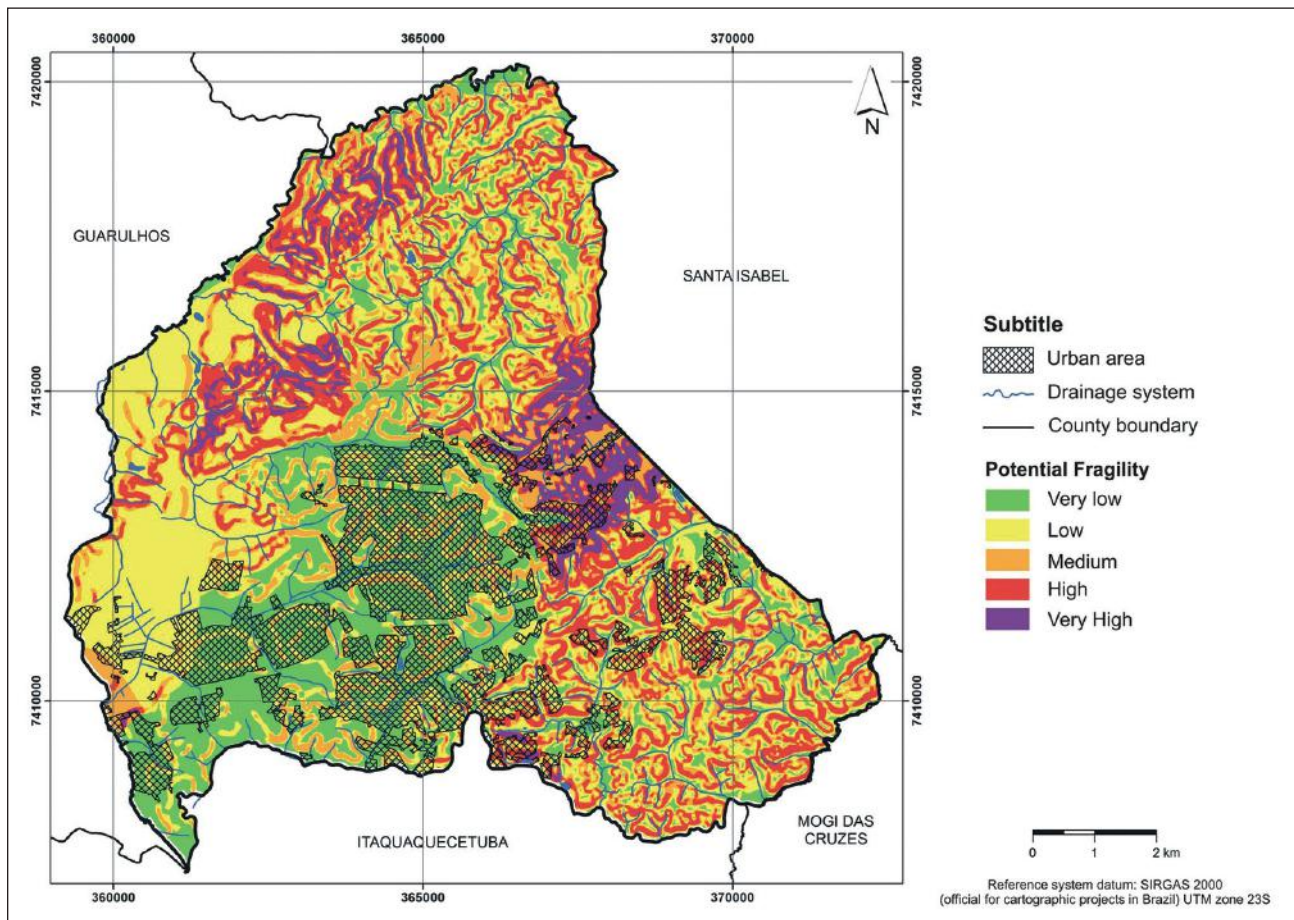


Figure 3 Potential Fragility Map of the Municipality of Arujá.

least preserved areas, taking into consideration the region with high anthropic densification, which is the most impacted. Such analyses were adapted and are essential as important instrument of evaluation of the physical-natural environment, considering the urban transformations, as shown by Santos and Ross (2012).

Therefore, the Emerging Fragility Map (Figure 4) presents regions with intense urban densification, as the central and eastern portion of the municipality, where fragility is unstable.

54.57 km² of the area of the Municipality of Arujá (55.86% of the total area) are inserted in very low to low fragility areas, showing a concentration of the arboreal cover and herbaceous vegetation respectively; the medium fragility areas correspond to 33.79% of the municipality area; the southeastern region – because it is a region close to the Presidente

Dutra Highway, is of high fragility and corresponds to 8.38%; and the regions that present very high fragility (1.97%) are those concentrated on the eastern border, between the road that links the Arujá and Santa Isabel municipalities and the Presidente Dutra and Mogi-Dutra highways.

Table 8 show that the Potential Fragility Map presents larger areas of very low, high and very high fragilities, when compared to the Emerging Fragility Map, due to the fact that declivity is associated with both cases, directly influencing the instability of the fragilities caused by urban densification.

In the analysis of the Emergent Fragility, the larger featured areas were the low and medium classes in relation to the Potential Fragility. When there is information on the anthropic concentration occurring these classes, the regions present a greater and mixed distribution.

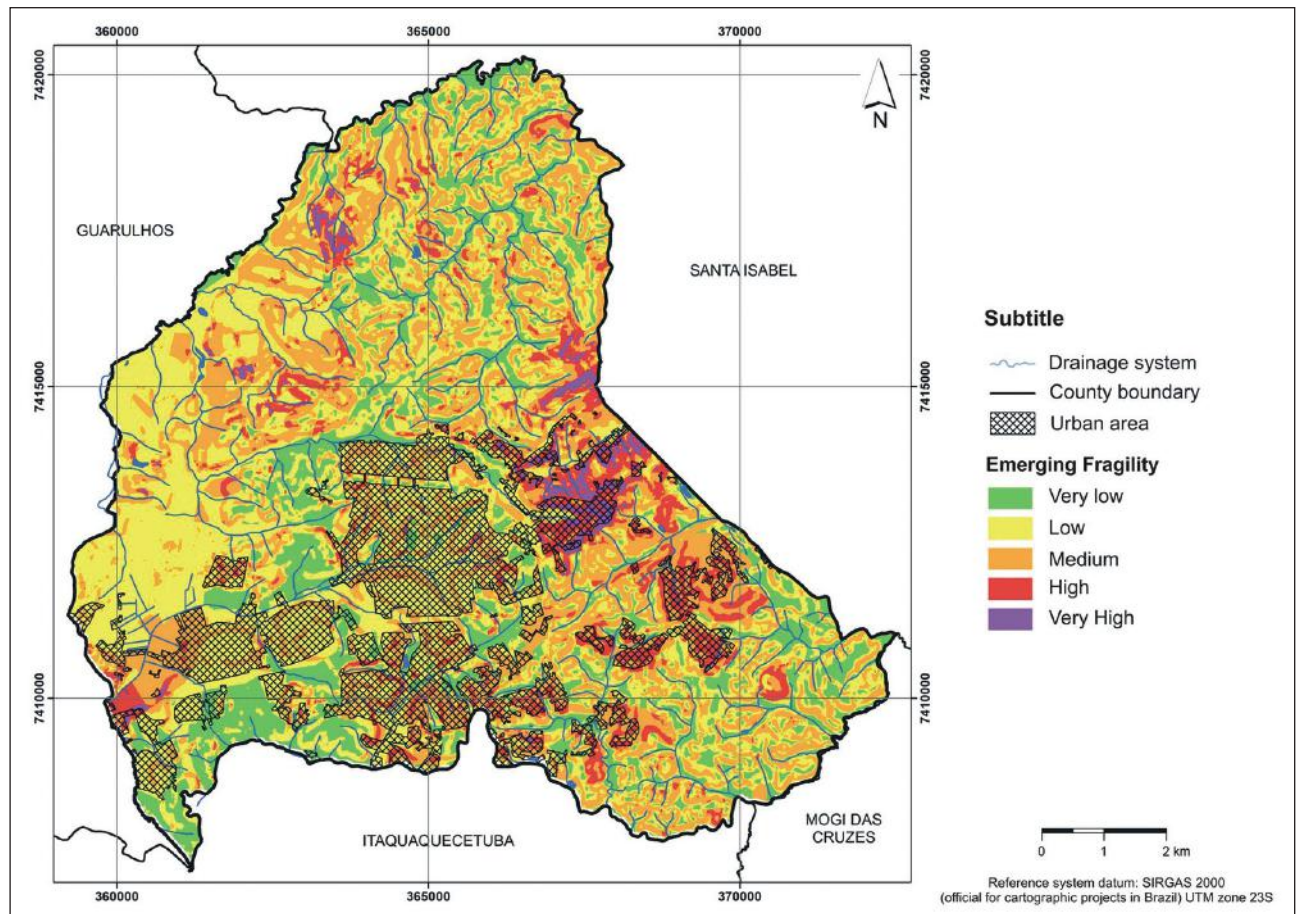


Figure 4 Emerging Fragility Map of the Municipality of Arujá.

FRAGILITY LEVELS	PF%	EF%
Very Low	24.11	16.49
Low	33.02	39.37
Medium	19.75	33.79
High	17.98	8.38
Very High	5.14	1.97
Total	100	100

Table 8 Potential (PF) and Emerging (EF) Fragility areas of the Municipality of Arujá.

4.3 Mean Surface Temperature Map

The surface temperature map prepared for this study presents three regions with minimum 21°C and maximum 37°C surface temperatures, as follows:

Region 1 – Northern Region, with arboreal and grass cover, water bodies, exposed soil and significant urban areas (small farms).

Region 2 – Central Region with the predominance of dense, consolidated, ordered and disordered urbanization.

Region 3 – Southern/Western Region, where an urban area with large condominiums and industry predominates.

The highest temperatures in the Arujá Municipality are associated with the most urbanized regions. This correspondence is very clear, mainly in the urban cloud of the Central/Western Region. Such correspondence is analyzed according to the methodology used by Barros & Lombardo (2016), who present the descriptive analysis, followed by the comparative analysis and finally by the integrated descriptive analysis. The adopted variables were the foliar area index, surface temperature, soil use patterns and the thermal classification of the urban heat island.

The land use characterization helps understand the change of the city climatic surface (Melaas *et al.*, 2016). It indicates that the thermal map thus prepared is reliable enough for a land use analysis and its implications in terms of thermal radiation.

The occurrence of high temperatures in the northern and northeastern portions that do not cor-

respond to urban areas reveals that such portions are occupied by rural activities, with the higher temperatures tending to occur in agricultural areas.

On the other hand, lower temperatures are associated with the massive presence of arboreal cover and water bodies in the study area. However, the factors water, altitude and forest can undergo the interference of other factors, because a cloud corresponding to a slight temperature increase in relation to the surrounding vegetated areas was observed, indicating the necessity to investigate the causes that can be related to the insolation incident on the escarpment facing eastwards and that corresponds to the time of information acquisition by the satellite Landsat-8 thermal sensor on September 25, 2015.

Figure 5 presents the combination of the analysis of the temperature and land use maps of the study area. This match clearly presents the direct relationship between urban densification and high temperatures, forming a heat island, which can be explained by the fact that materials used in constructions store heat. This explanation is based on Bias *et al.* (2003) and Teza & Baptista (2005). The vegetation concentration coincides with low temperatures, promoted by evapotranspiration performed by plants. The process allows heat propagation and storage to take place in environments where exchange via transpiration is not possible, such as urban regions that present materials that absorb heat (Barros & Lombardo, 2016).

In Figure 6, the principal component analysis showed that in Component 1, EF has a positive correlation with mean and high values at surface temperature and with Land use, especially in urban areas (red circle). The yellow and red dots marked within the circle suggest that the parameters of land use, as well as LST, are important indicators of areas with medium and high emergent fragility, especially in urban areas or in those with little or no vegetation cover (exposed soil). On the other hand, in Component 2, high slope values are associated with areas with high PF values (red dots in the black circle). However, other parameters such as geology and soils, remained neutral in both main components, demonstrating a low influence of these parameters in the values of fragility.

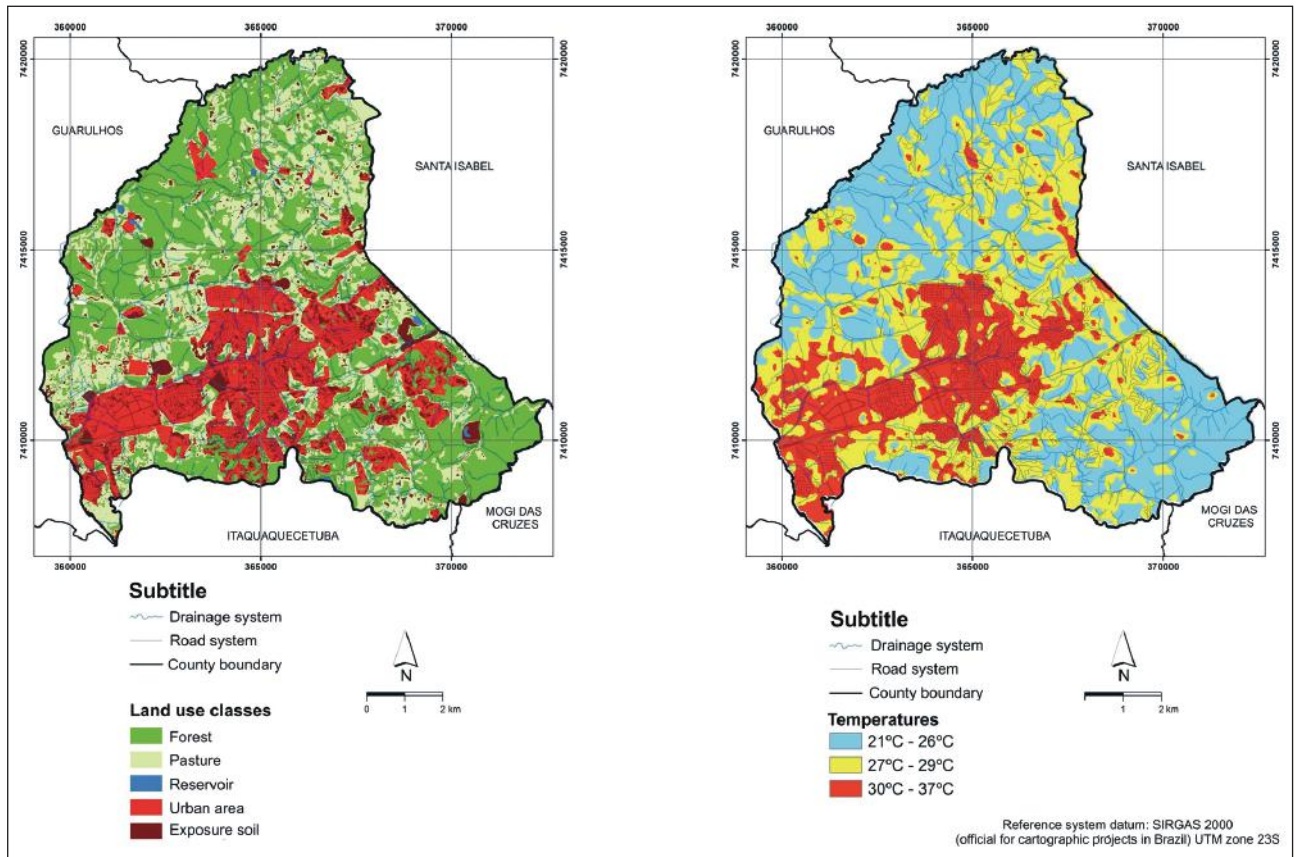


Figure 5 Land Use map (left) X Thermal map (right).

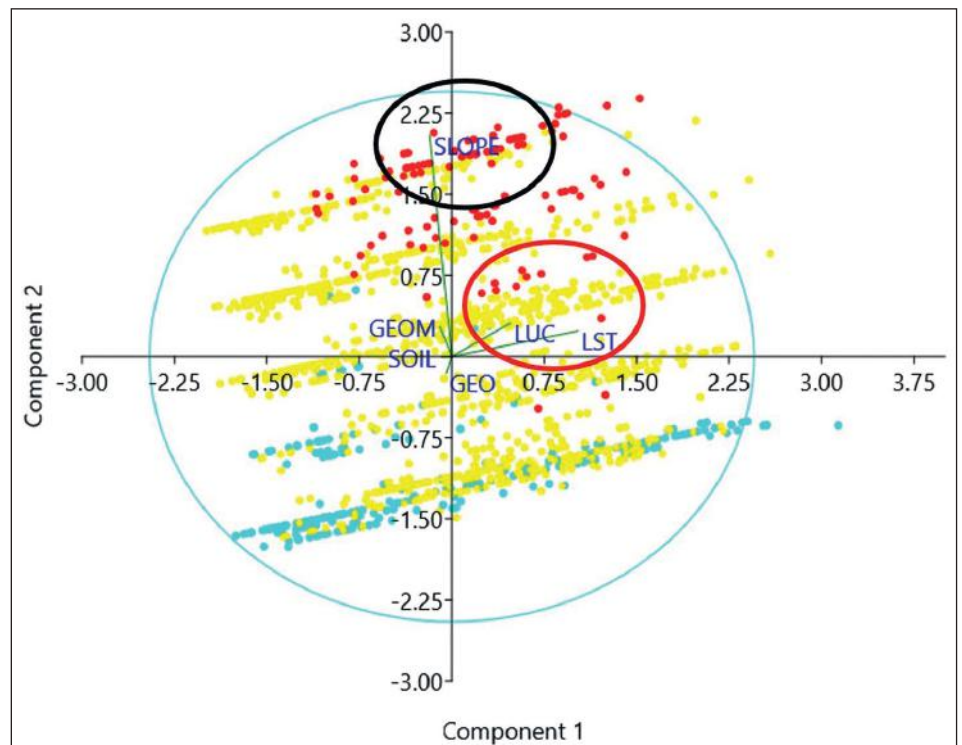


Figure 6 Scatter plot for the Emerging and Potential Fragilities X Physical parameters and land surface temperature.

In this context, the presence of vegetation is capable of improving the environmental quality, promoting the ecological equilibrium and reduction of environmental fragility (Boone *et al.*, 2012; Cai-che *et al.*, 2016).

Alcamo *et al.* (2003) consider the thermal images indicators of the presence or lack of thermal comfort conditions made available by the vegetation by means of thermal regulation for human well-being. Therefore, the removal of the vegetation cover is one of the factors that change the city climate. As pointed by Romero (2001) and Sorre (2006), besides climatic changes caused by urbanization, the replacement of the vegetation by constructions, contributes to the decrease of water infiltration in the soil and runoff.

By means of varied infra-red radiation behavior and heat emission by objects, the satellite thermal images identify the areas of the Earth's surface of different surface temperatures (Weng, 2009). These images present very important correlations with land use (Buyantuyev & Wu, 2010; Zhou *et al.*, 2011) and reveal areas with more or less vegetation cover (Deng & Wu, 2013).

The formation of heat islands in the cities, according to Lombardo (1985) and Coltri *et al.* (2007), results from changes of solar energy flows that reach the soil surface by means of physical processes, changing some meteorological elements, in special surface and air temperatures. Heating is more intense during the day, due to the capacity of thermal absorption of the building materials used in the city, which give back part of the radiation to the atmosphere.

Studies by Blain *et al.* (2009) in three cities in the State of São Paulo, and Xavier *et al.* (2009) in Cuiabá – MT indicate that both surface and air temperature have changed during urban expansion, being a result of little afforestation and greater density of buildings.

In Brazil, Lombardo (1985), presenting one of the first studies on the subject, identified soil occupation elements and showed an increase in surface temperature by means of satellite images, relat-

ing this increase to urbanization. Cunha, Rufino & Ideião (2009) studied the relationship between urban growth and the increase in air and surface temperature in Campina Grande (State of Paraíba), on the basis of remote sensing techniques that monitor possible changes in local climate.

Coltri *et al.* (2007) identified a heat island in Piracicaba (State of São Paulo) by means of geoprocessing techniques and satellite images. It was concluded that the green area size in a city determines the heat island intensity. The study that Feitosa *et al.* (2011) carried out in Teresina shows that in 20 years the vegetated areas have been reduced as the population grew and the city expanded. When checking the temperatures of the soil surface, these were higher in the regions of higher concentration of built areas. In the periphery where green areas are more abundant, the temperatures are milder, which indicates that urban expansion can influence air temperature and alter the climatic trends.

Lombardo (1985) describes important parameters to characterize and determine the heat island intensity: decrease in evaporation (lack of vegetation and available water); solar radiation that is not used in evaporation is spent in heating the city streets, buildings and air;

- increase in rugosity (presence of buildings), increasing turbulence, which helps transfer heat upwards, at the same time that zonal runoff diminishes; quantity of exposed soil, which increases the surface temperature; the topography of the city, where mountains and valleys can act as barriers for hot air dispersion; and the thermal properties of the buildings and paving materials that absorb energy during the day; at night they emit long-wave radiation, causing higher temperatures during the night than during the day.

Studies such as Li *et al.* (2014), Lin *et al.* (2015) and Mohan & Kandya (2015) were carried out using information from thermal bands of satellite images Landsat-8 which showed varied factors that influenced the surface temperature variation, such as: presence or absence of vegetal cover; the relief and its orientation; atmospheric conditions; urbanized vs. non-urbanized areas; occupation patterns in urban areas.

5 Conclusions

The urban area of the Municipality of Arujá is inserted in areas of very low and low Potential Fragility, due to the predominance of mounds, declivities between 6 and 20 %, and geologically characterized by gneisses and granites. In the central/eastern and northwestern regions of the municipality there are areas of very high Potential Fragility because of the influence of the relief characterized by high hills.

Regarding the Emerging Fragility, the urban area is inserted in a low to medium fragility zone, which is a more critical situation than in Potential Fragility, due to the negative influence exerted by the urban facilities themselves. As with the Potential Fragility map, areas of very high Emerging Fragility are localized in the central/eastern and northwestern zones of Arujá, but in a smaller area.

Regarding the fraction of each fragility class in relation to the total area of the municipality, classes “very low” and “low” are very similar, corresponding to 57.13% and 55.86 % in the Potential Fragility and Emerging Fragility maps respectively. A larger difference is seen for medium fragility (19.75% and 33.79% in the Potential Fragility and Emerging Fragility maps respectively); high fragility (17.98% and 8.38% in the Potential Fragility and Emerging Fragility maps respectively); and very high fragility classes (5.14% and 1.97% in the Potential Fragility and Emerging Fragility maps respectively).

The thermal map of the Municipality of Arujá confirms what has been published in the technical literature, that the urban areas present higher temperatures than the rural or non-urbanized areas, due to heating of the structures that compose the central areas (asphalt, concrete and roofs) and sparse vegetation. Vegetation could decrease the temperature by evapotranspiration from leaves and because the canopy of trees does not have the characteristic of storing the heat of the sun.

All the data represented both in the Potential and Emerging Fragility maps can be used as important tools in the preparation or renovation of the Municipal Director Plans, because they show the areas that the Public Power should give more attention to,

when it comes to geotechnical and environmental problems, providing vectors for possible expansion of the urban area and taking into account green areas (linear parks and larger grassed areas on private lawns and sidewalks).

In conclusion, it is suggested that the Public Power analyze such surveys in order to elaborate an action plan to mitigate the impacts caused by intense urbanization in the region. Besides, the reformulation of the Municipal Director Plan is suggested, focusing on the conservation of the municipality rich biodiversity by means of a proper urban planning.

6 Acknowledgments

To CAPES for the Master's Scholarship (PROSUP - Programa de Apoio à Pós-Graduação em Instituições de Ensino Particular) granted to Bruna Daniele de Carvalho Gimenez Torresani.

7 References

- Alcamo, J. 2003. Ecosystems and human well-being: a framework for assessment. Washington, D.C., USA, Island Press. 245p.
- Andrade, M.R.M.; Oliveira, A.M.S.; Queiroz, W. Sato, S. E.; Barros, E.J.; Bagattini, G. & Aleixo, A.A. 2008. Aspectos fisiográficos da paisagem guarulhense, In: OMAR, E (org.). Guarulhos Tem História Questões Sobre História Natural, Social E Cultural. Editora Ananda. São Paulo. p. 25-37.
- Barros, H.R. & Lombardo, M.A. 2016. A ilha de calor urbana e o uso e cobertura do solo em São Paulo-SP. *Geosp – Espaço e Tempo*, 20(1): 160-177.
- Bias, E.S.; Baptista, G.M.M. & Lombardo, M.A. 2003. Análise do fenômeno de ilhas de calor urbanas, por meio da combinação de dados landsat e ikonos. In: SIMPÓSIO BRASILEIRO DE SENSORIAMENTO REMOTO, 11. Belo Horizonte, 2003. p. 1741 – 1748.
- Blain, G.C.; Picoli, M.C.A. & Lulu, J. 2009. Análises estatísticas das tendências de elevação nas séries anuais de temperatura mínima do ar no estado de São Paulo. *Bragantia*, 68(3): 807-815.
- Boone, C.G.; Cook, E.; Hall, S.J.; Nation, M.L.; Grimm, N.B.; Raish, C.B.; Finch, D.M. & York, A.M. 2012 A comparative gradient approach as a tool for understanding and managing urban ecosystems. *Urban Ecosystems*, 15: 795-807.
- Buyantuyev, A. & Wu, J. 2010. Urban heat islands and landscape heterogeneity: Linking spatiotemporal variations in surface temperatures to land-cover and socioeconomic patterns. *Landscape Ecology*, 25 (1): 17–33.
- Caiche, D.T.; Silva, S.R.M.; Viana, S.M. & Silva, R.S. 2016. Análise da supressão da arborização viária da cidade de São Carlos/SP no período de 2004 a 2013. *Revista da Sociedade Brasileira de Arborização Urbana*, 11(3): 93-103.
- Coltri, P.P.; Fagnani, M.A.; Labaki, L.C.; Ferreira, N.J. & Demétrio, V.A. 2007. Variabilidade dos principais elementos climáticos e urbanização na região de Piracicaba (SP). Bra-

- zilian *Journal of Biosystems Engineering*, 1(2): 197-208.
- Crepani, E.; Medeiros, J.S.; Hernandez Filho, P.; Florenzano, T.G.; Duarte, V. & Barbosa, C.C. F. 2001. Sensoriamento remoto e geoprocessamento aplicado ao zoneamento ecológico-econômico e ao ordenamento territorial. INPE-8454-R-PQ/722. São José dos Campos. 111p.
- Cunha, J.E.B.L.; Rufino, I. A.A. & Ideião, S.M.A. 2009. Determinação da temperatura de superfície na cidade de Campina Grande-PB a partir de imagens do satélite Landsat 5-TM. In: SIMPÓSIO BRASILEIRO DE SENSORIAMENTO REMOTO, 14, Natal. 2009. Anais. p. 5717-5724.
- Deng, C. & Wu, C. 2013. Examining the impacts of urban biophysical composition on surface urban heat island: A spectral unmixing and thermal mixing approach. *Remote Sensing of Environment*, 131: 262–274.
- Eastman, J. R. 2006. *Idrisi Andes: Guide to GIS and Image Processing*. Clark University, Worcester. 328p.
- ESRI - Environmental Systems Research Institute. 2011. *ArcGIS Desktop: Release 10*. Redlands, CA: Environmental Systems Research Institute.
- Feitosa, S.M.R.; Gomes, J.M.A.; Neto, J.M.M. & Andrade, C.S.P. 2011. Consequências da Urbanização na Vegetação e na Temperatura da Superfície de Teresina – PIAUI. *Revista da Sociedade Brasileira de Arborização Urbana*, 6(2): 58-75.
- IBGE – INSTITUTO BRASILEIRO DE GEOGRAFIA E ESTATÍSTICA. 2011. *Censo Demográfico do Estado de São Paulo do ano de 2010*. São Paulo.
- IBGE – INSTITUTO BRASILEIRO DE GEOGRAFIA E ESTATÍSTICA. 2018. *Cidades Arujá 2014*. Available in: <www.ibge.gov.br/cidadesat/xtras/perfil.php?codmun=350390>. Accessed on 07/01/2018.
- Klais, T.B.A.; Dalmas, F.B.; Morais, R.P.; Atique, G.; Lastoria, G. & Paranhos Filho, A.C. 2012. Vulnerabilidade natural e ambiental do município de Ponta Porã, Mato Grosso do Sul, Brasil. *Revista Ambiente & Água*, 7(2): 277-290.
- Li, W.; Bai, Y.; Chen, Q.; He, K.; Ji, X. & Han, C. 2014. Discrepant impacts of land use and land cover on urban heat islands: A case study of Shanghai. *China. Ecological Indicators*, 47: 171–178.
- Lin, W.; Yu, T.; Chang, X.; Wu, W. & Zhang, Y. 2015. Calculating cooling extents of green parks using remote sensing: Method and test. *Landscape and Urban Planning*, 134: 66-75.
- Lombardo, M.A. 1985. *Ilhas de Calor nas Metrópoles: o exemplo de São Paulo*. São Paulo. Editora Hucitec. 224p.
- Massa, E.M. & Ross, J.L.S. 2012. Aplicação de um modelo de Fragilidade Ambiental relevo – solo na Serra da Cantareira, Bacia do Córrego do Bispo, São Paulo – SP. *Revista do Departamento de Geografia – USP*, 24: 57–79.
- Mellas, E.K.; Wang, J.A.; Miller, D.L. & Friedl, M.A. 2016. Interactions between urban vegetation and surface urban heat islands: a case study in the Boston metropolitan region. *Environmental Research Letters*, 11(5): 1-11.
- Mohan, M. & Kandya, A. 2015. Impact of urbanization and land-use/land-cover change on diurnal temperature range: A case study of tropical urban airshed of India using remote sensing data. *Science of The Total Environment*, 506: 453–465.
- PMA – Prefeitura Municipal de Arujá. *Plano Municipal de Saneamento. Sistemas de abastecimento de água e de esgotamento sanitário*. Município de Arujá, 2012. Available in: <http://www.prefeituradearuja.sp.gov.br/legislacao/obras/PlanoMunicipalDeSaneamento.pdf>. Accessed on 24/01/2018.
- Ribeiro, T.F.B. 2016. *Reflexos do Uso da Terra na Avaliação da Poluição Hídrica da Bacia Hidrográfica do Ribeirão das Lavras, Guarulhos – SP*. Programa de Pós-Graduação em Análise Geoambiental, Universidade Guarulhos, Dissertação de Mestrado, 122 p.
- Romero, M.A.B. 2001. *A arquitetura bioclimática do espaço público*. Ed. UNB. Coleção arquitetura e urbanismo. Brasília. 225 p.
- Ross, J.L.S. 1990. *Geomorfologia Ambiente e planejamento*. São Paulo. Editora Contexto. 85p.
- Ross, J.L.S. 1994. Análise Empírica da Fragilidade dos Ambientes Naturais e Antropizados. *Revista do Departamento de Geografia (USP)*, 8: 63-74.
- Ross, J.L.S. 1995. Análises e Sínteses na Abordagem Geográfica da Pesquisa para o Planejamento Ambiental. *Revista do Departamento de Geografia da USP*, 9: 65-75.
- Ross, J.L.S. & Moroz, I.C. 1996. Mapa Geomorfológico do Estado de São Paulo. *Revista do Departamento de Geografia da USP*, 10: 41-58.
- Santos, J.O. 2006. *Vulnerabilidade ambiental e áreas de risco na Bacia hidrográfica do rio*
- Cocó: Região Metropolitana de Fortaleza. Programa de Pós-Graduação em Geografia. Universidade Federal do Ceará. Dissertação de Mestrado, 216 p.
- Santos, J.O. 2015. *Relações entre Fragilidade Ambiental e Vulnerabilidade Social na Susceptibilidade aos Riscos*. Mercator, 14(2): 75-90.
- Santos, J.O. & Ross, J. L.S. 2012. *Fragilidade Ambiental Urbana*. *Revista da Associação Nacional de Pós-Graduação e Pesquisa em Geografia*, 8(10): 127-144.
- Silveira, T.; Rego, N.A.C.; Santos, J.W.B. & Araújo, M.S.B. 2014. *Qualidade da Água e Vulnerabilidade dos Recursos Hídricos Superficiais na Definição das Fragilidades Potencial e Ambiental de Bacias Hidrográficas*. *Revista Brasileira de Geografia Física*, 7(4): 642-652.
- Sorre, M. 2006. *Objeto e método da climatologia*. *Revista do Departamento de Geografia da Universidade de São Paulo*, 18: 89-94.
- Teza, C.T.V. & Baptista, M.M.de. 2005. Identificação do fenômeno ilhas urbanas de calor por meio de dados ASTER. In: SIMPÓSIO BRASILEIRO DE SENSORIAMENTO REMOTO, 12, Goiânia, Brasil. Anais, p. 3911-3918.
- Tricart, J. 1977. *Ecodinâmica*. Rio de Janeiro: Instituto Brasileiro de Geografia e Estatística. 91p.
- USGS - United States Geological Survey. *LANDSAT 8 (L8) DATA USERS HANDBOOK*. Available on: <<http://landsat.usgs.gov/documents/Landsat8DataUsersHandbook.pdf>>. Accessed in 24/11/2017.
- Viezzler, J.; Biondi, D.; Batista, A.C. & Brandt, D. 2016. Perfil dos usuários e sua percepção dos elementos de composição paisagística das praças de Curitiba – PR. *Revista da Sociedade Brasileira de Arborização Urbana*, 11(3): 01-16.
- Voogt, J.A. & Oke, T.R. 2003. Thermal remote sensing of urban climates. *Remote Sensing of Environment*. 86: 370–384.
- Weng, Q. 2009. Thermal infrared remote sensing for urban climate and environmental studies: Methods, applications, and trends. *Journal of Photogrammetry and Remote Sensing*, 64(4): 335–344.
- Xavier, A.L.; Nogueira, M.C.J.; Maitelli, G.T.; Oliveira, A.G.; Oliveira, A.S.; Santos, F.M.M. & Nogueira, J.S. 2009. Variação de temperatura e umidade entre áreas urbanas de Cuiabá. *Engenharia Ambiental*, 6: 82-93.
- Zhou, W.; Huang, G. & Cadenasso, M.L. 2011. Does spatial configuration matter? Understanding the effects of land cover pattern on land surface temperature in urban landscapes. *Landscape and Urban Planning*, 102 (1): 54–63.